

PAPER • OPEN ACCESS

Multi-electron beam generation using co-propagating, parallel laser beams

To cite this article: J Elle *et al* 2018 *New J. Phys.* **20** 093021

View the [article online](#) for updates and enhancements.



IOP | ebooks™

Bringing you innovative digital publishing with leading voices to create your essential collection of books in STEM research.

Start exploring the collection - download the first chapter of every title for free.



PAPER

Multi-electron beam generation using co-propagating, parallel laser beams

OPEN ACCESS

RECEIVED

21 March 2018

REVISED

15 August 2018

ACCEPTED FOR PUBLICATION

4 September 2018

PUBLISHED

19 September 2018

Original content from this work may be used under the terms of the [Creative Commons Attribution 3.0 licence](#).

Any further distribution of this work must maintain attribution to the author(s) and the title of the work, journal citation and DOI.



J Elle¹, T Z Zhao², Y Ma², K Behm², A Lucero¹, A Maksimchuk², J A Nees², A G R Thomas²,
A Schmitt-Sody¹ and K Krushelnick^{2,3}

¹ Air Force Research Laboratory, Kirtland AFB, Albuquerque, NM, United States of America

² Center for Ultrafast Optical Science, University of Michigan Ann Arbor, 48109, United States of America

³ Author to whom any correspondence should be addressed.

E-mail: kmkkr@umich.edu

Keywords: lasers, accelerators, plasmas, particle sources

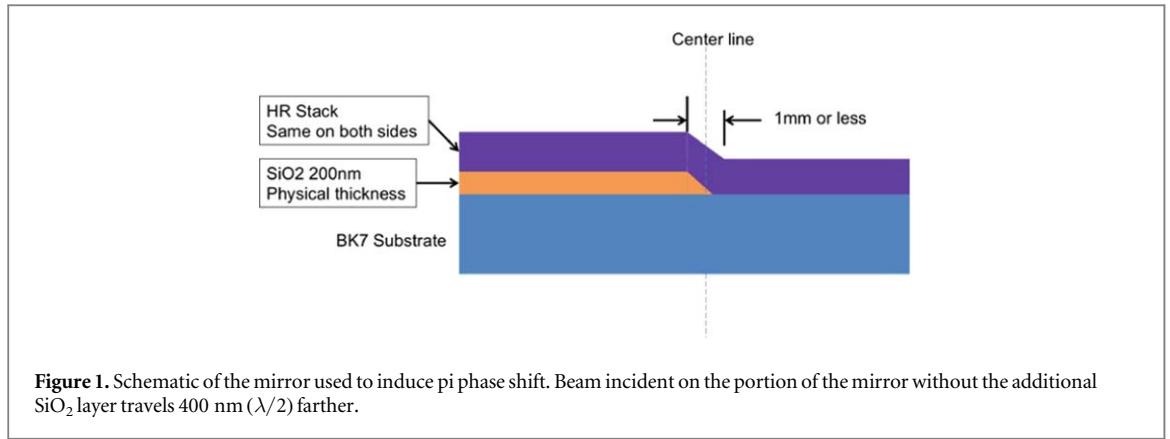
Abstract

High intensity short pulse laser plasma interaction experiments were performed to investigate laser wakefield acceleration (LWFA) in the ‘bubble’ regime. Using a specially designed phase plate, two high intensity laser focal spots were generated adjacent to each other with a transverse spacing of 70 μm and were focused onto a low density plasma target. We found that this configuration generated two simultaneous relativistic electron beams from LWFA (with low divergence) and that these beams often interact strongly with each other for longer propagation distances in the plasma thus reducing beam quality. In addition, it was observed that the existence of an adjacent laser driven wakefield significantly reduced the self-trapping threshold for injection of electrons. Numerical modeling of these interactions demonstrated similar phenomena and also showed that electron beam properties can be affected through precise control of the phase and polarization of the incident laser beam.

Laser wakefield acceleration (LWFA) promises to greatly reduce the size and cost of future particle accelerators. Significant improvements in the quality of relativistic electron beams from laser wakefield experiments have been made over the past few years. In 2004, mono-energetic electron beams were generated for the first time [1–3] and several years later the generation of GeV energy range electron beams using centimeter length plasmas [4–6] was demonstrated. The stability and control of the process for injecting bursts of electrons into these plasma accelerating structures [7] has also been improved using a variety of methods such as colliding pulse injection [8], density gradient injection [9], and ionization injection [10, 11]. These advances have demonstrated the feasibility of using plasma-based accelerators for a variety of applications. However, challenges still remain to increase the total charge of the accelerated electron beams and to control beam parameters such as emittance, dark current, and energy spread. Current experimental results show that the maximum accelerated charge ranges from several tens of pC to about 1 nC. For applications in high-energy density physics, beam-driven inertial confinement fusion, and high-flux radiation sources, large beam charge is beneficial, and is often a critical requirement.

The accelerated charge in LWFA experiments is affected by a number of factors such as beam loading, propagation distance, ionization-induced defocusing of the laser pulse, and other factors due to the specific injection method used [12]. More charge can typically be obtained simply by lowering the plasma density. However, lowering the density in this way also requires a higher laser power for self-focusing, trapping and accelerating electrons. If higher laser power is available, this is the most straightforward way to increase the overall charge.

It has been suggested that a potentially more efficient method of increasing the charge, using fixed laser energy, is to generate two wakefields that co-propagate simultaneously and which independently inject charge into each wakefield [13]. Previous simulation work [13] indicated that the total number of accelerated electrons can be increased in LWFA by using multiple parallel laser pulses; the amount of accelerated charge was observed in these simulations to increase linearly with the number of laser pulses. Such increased beam charge can then



also potentially lead to an increase in radiation emission (from THz emission to hard x-rays resulting from ‘betatron’ oscillations [14]). However for implementation of such experimental configurations, it is necessary to understand how multiple parallel laser beams can generate multiple wakefields and whether adjacent wakefield structures can interact and be controlled.

Simultaneous parallel laser beams can be created experimentally in a number of ways. For example, if the laser beam quality is non-uniform, the focal spot of a single beam can naturally evolve from a single spot to a double spot within the Rayleigh length of the focusing optic and create two beams resulting from a self-focusing instability in the plasma [15]. This method, of course, may not exist for every experimental setup. However, a more reliable way to generate two beams is to use a mirror with a step discontinuity to change the phase of half of the single beam in the near-field by π radians as shown in figure 1. The resulting laser beam is quasi-radially polarized with a TEM₀₁ far field mode, generating two focal spots of approximately equal energy. In the experiments described here we have implemented this setup using interferometry to verify the phase shift.

In this paper, the charge and energy of relativistic electron beams generated using such dual focal spots are characterized and compared with those generated using a single focal spot with similar total pulse energy or with a single spot with pulse energy corresponding to only one of the focal spots (i.e., half energy). A π phase shift mirror is used to create two stable laser spots at focus. Our experiments showed that, although two separate electron beams were consistently generated, a significant increase in the electron beam charge produced by two adjacent laser beams was not observed when compared to a single beam having the same total energy. However, there was a significant reduction in the self-trapping (self-injection) threshold for these beams and there was also often an increase in the overall divergence of the electron emission due to interaction of the two electron beams with each other during propagation such that a resulting beam hosing [16] or ‘beam-braiding’ instability could be observed.

In these experiments, a 10 cm diameter π -phase shift mirror at near normal incidence was inserted in the beam path of the HERCULES laser system [17] at the University of Michigan at the entrance of the target chamber and an additional 12.5 cm diameter silver mirror redirected the beam to a 2 m focal length off-axis parabolic mirror used for laser wakefield experiments. LWFA experiments were performed using a 3 mm single stage gas cell target [18] with a laser power up to 55 TW ($\lambda = 800$ nm, $\tau = 30$ fs). For the focal spot sizes in this work, this corresponds to a peak intensity of approximately 7×10^{18} W cm⁻² ($a_0 \sim 2$). Both mixed gas (97.5% He and 2.5% N₂ gas mixture) and pure helium gas were used in the cell for the plasma target. No significant difference between these gases was noted for the main results of these experiments as described below. An electron spectrometer using a permanent magnet was used to measure the electron beam energy and charge. Transverse interferometry was used to measure plasma electron density.

The focal spots were characterized using a CCD camera. Figures 2 and 3 show typical images of the energy distribution for single and double focal spots, respectively, at various distances within the Rayleigh length (1.5 mm) of the focusing $f/20$ paraboloidal mirror. For the dual focal spots, there is typically a slightly uneven distribution of energy between the spots. This was because in our experiments the mirror step discontinuity was not perfectly centered, resulting in slightly more energy in the upper focal spot. We see later that this may lead to the production of dual electron beams that are slightly mismatched in either energy or charge.

Analyses of the focal spot images show that the full width at half maximum (FWHM) diameter of the single and double focal spots are approximately the same and were 28 μ m. In addition, the total energy in the FWHM of the dual focal spots is similar as compared with the energy contained in the FWHM of a single focal spot. The separation between the dual focal spots in the vertical direction is approximately 70 μ m.

Typical energy spectra of the electron beams generated using either a single or dual focal spots in the 3 mm single stage cell are shown in figure 4. The dotted vertical lines denote the energy of the beam as indicated starting

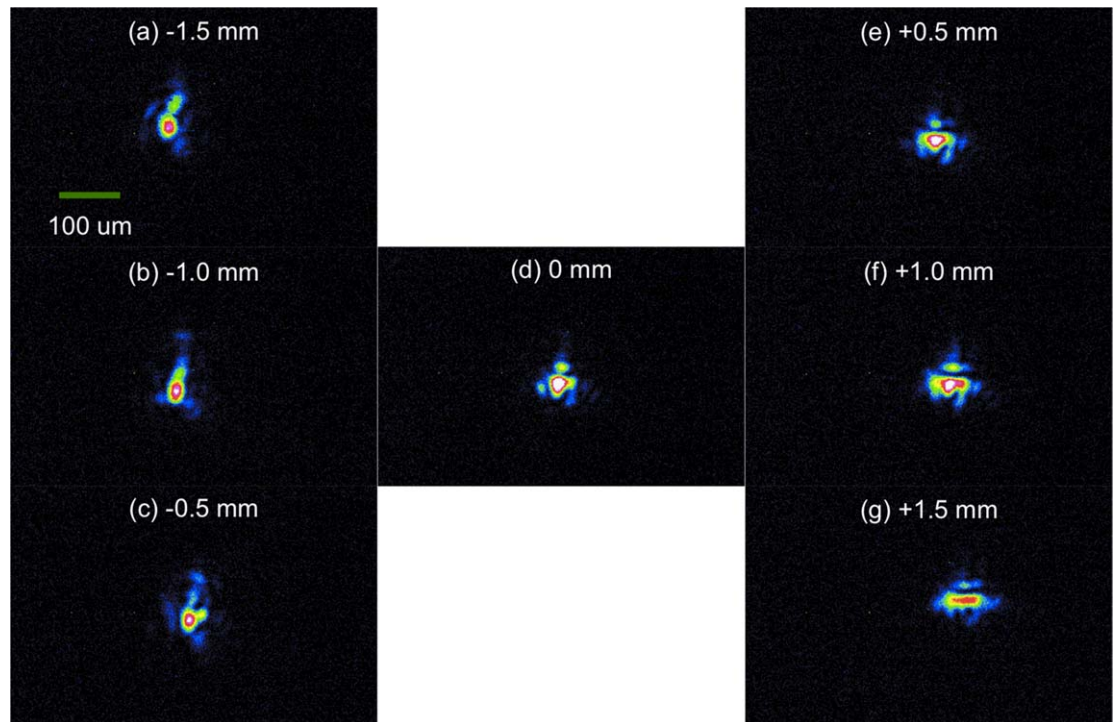


Figure 2. Representative images of the energy distribution within a single focal spot throughout the confocal length of the $f/20$ focusing optic. 0 mm denotes the position of best focus. Positive numbers denote positions after focus and vice versa for negative numbers.

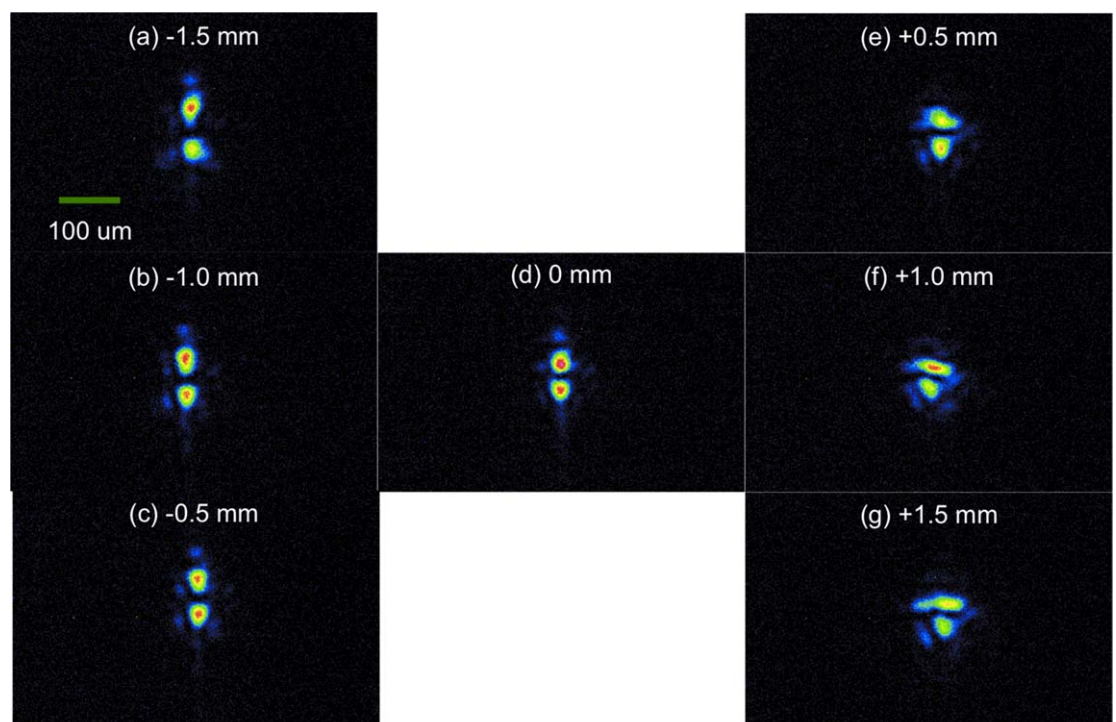
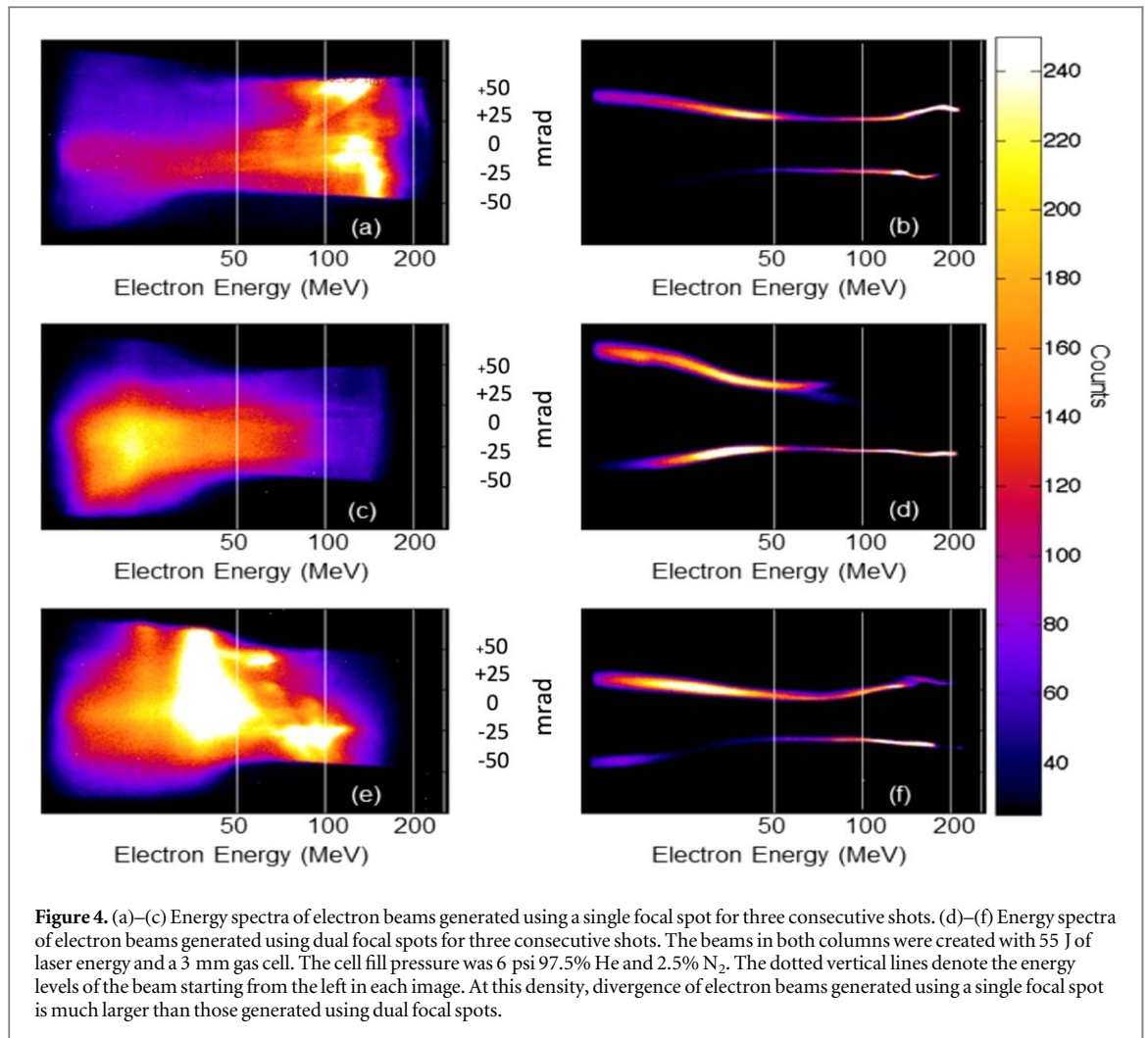
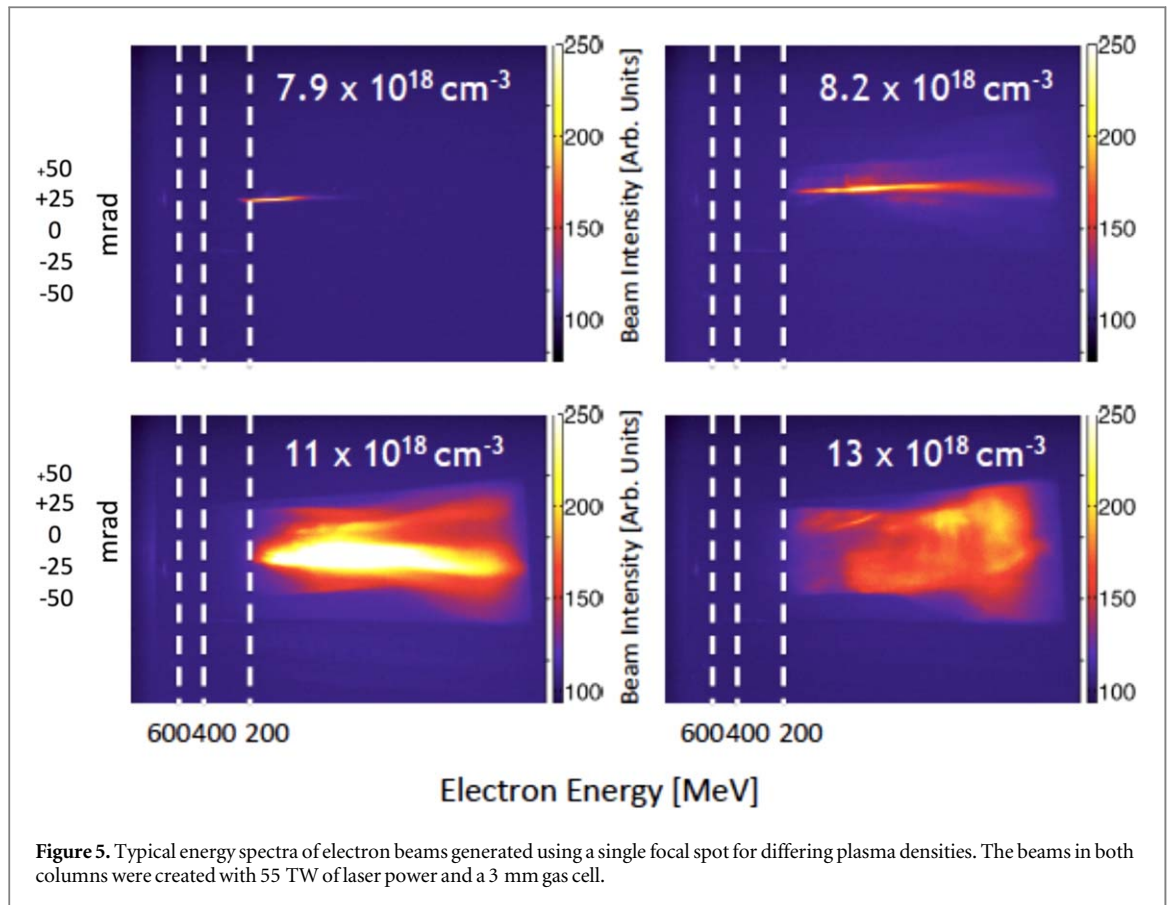


Figure 3. Representative images of the energy distribution within dual focal spots, generated using a coated mirror, throughout the confocal length of the $f/20$ focusing optic. A slight asymmetry in the energy distribution (weighted towards the top beam) can be seen for the dual focal spots. 0 mm denotes the position of best focus. Positive numbers denote positions after focus and vice versa for negative numbers.



from the right in each image. The spectra in both columns were generated using the same laser parameters, plasma density ($\sim 10^{19} \text{ cm}^{-3}$), and gas mix. In the case of a single electron beam, more charge is loaded into the wakefield bubble and as a result beam loading (and a reduction in charge injection) can occur at lower density. As a comparison the typical spectra of electron beams for single beams at 55 TW for this experiment with respect to changing density is shown in figure 5. For a plasma density below about $8 \times 10^{18} \text{ cm}^{-3}$, the single electron beam energy spectra demonstrate divergence as good or better than the individual dual beam divergence (figure 4). However, as density is increased to 10^{19} cm^{-3} the electron beam divergence in the single beam case has increased by an order of magnitude while the dual beams maintain a small individual divergence for similar total charge, as shown in figure 4. At higher densities such as $1.5 \times 10^{19} \text{ cm}^{-3}$ even the dual beam divergence has started to increase. In the case of dual electron beams, the maximum energy and charge between the two beams are not generally equal, potentially as a result of the uneven energy distribution in the two focal spots. It should be noted that the ‘hour-glass’ shaped feature at the low-energy end of the dual beam spectra in figure 4 is an artifact resulting from the interaction of lower energy electrons with the fringe fields of the dipole magnet inside the experimental chamber.

The energy spectra of the dual electron beams also showed interesting dynamics when a two-stage cell was used such that the laser/electron beam propagation was extended to longer lengths (beyond the dephasing distance) [12]. In figures 6(a)–(c), trajectory crossing between the two electron beams and significantly enhanced transverse oscillations of the electron beams can be observed. In figures 6(d)–(f), the formation of a third beam is observed whose energy and charge are comparable to the other two beams. The generation of the third beam only occurred in the two-stage cell due to the longer propagation distance available in the cell (6.5–11.5 mm). This suggests that there is an optimal length over which the two wakefields can fully develop and trap charge. For the laser pulse parameters and densities used when operating with the two-stage cell, dual beams were consistently generated for all lengths, in comparison to an 80% formation rate for the optimal electron density of $\sim 10^{19} \text{ cm}^{-3}$ in the 3 mm single-stage cell. The formation of the triple beams was less often observed and is likely due to the formation of a third wakefield in the region between the two main beams.

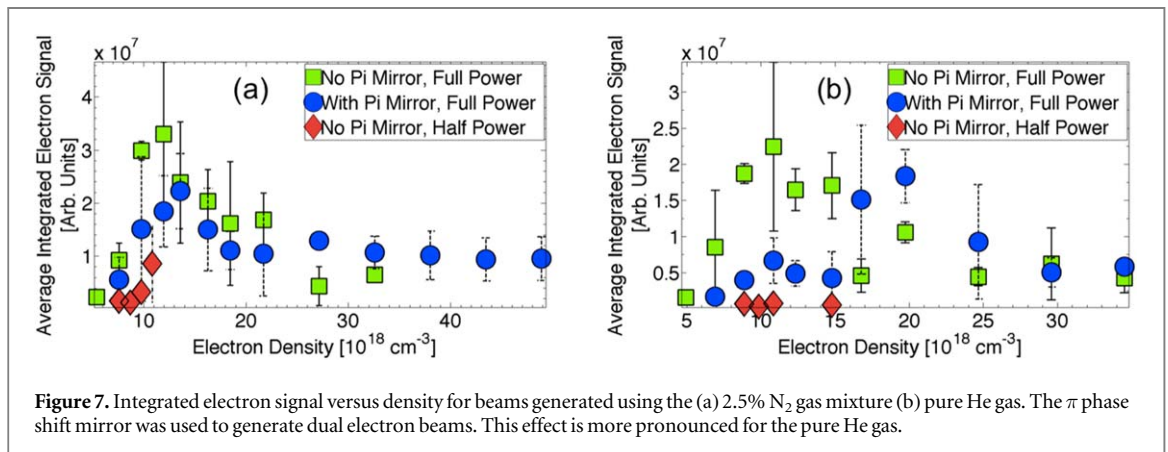
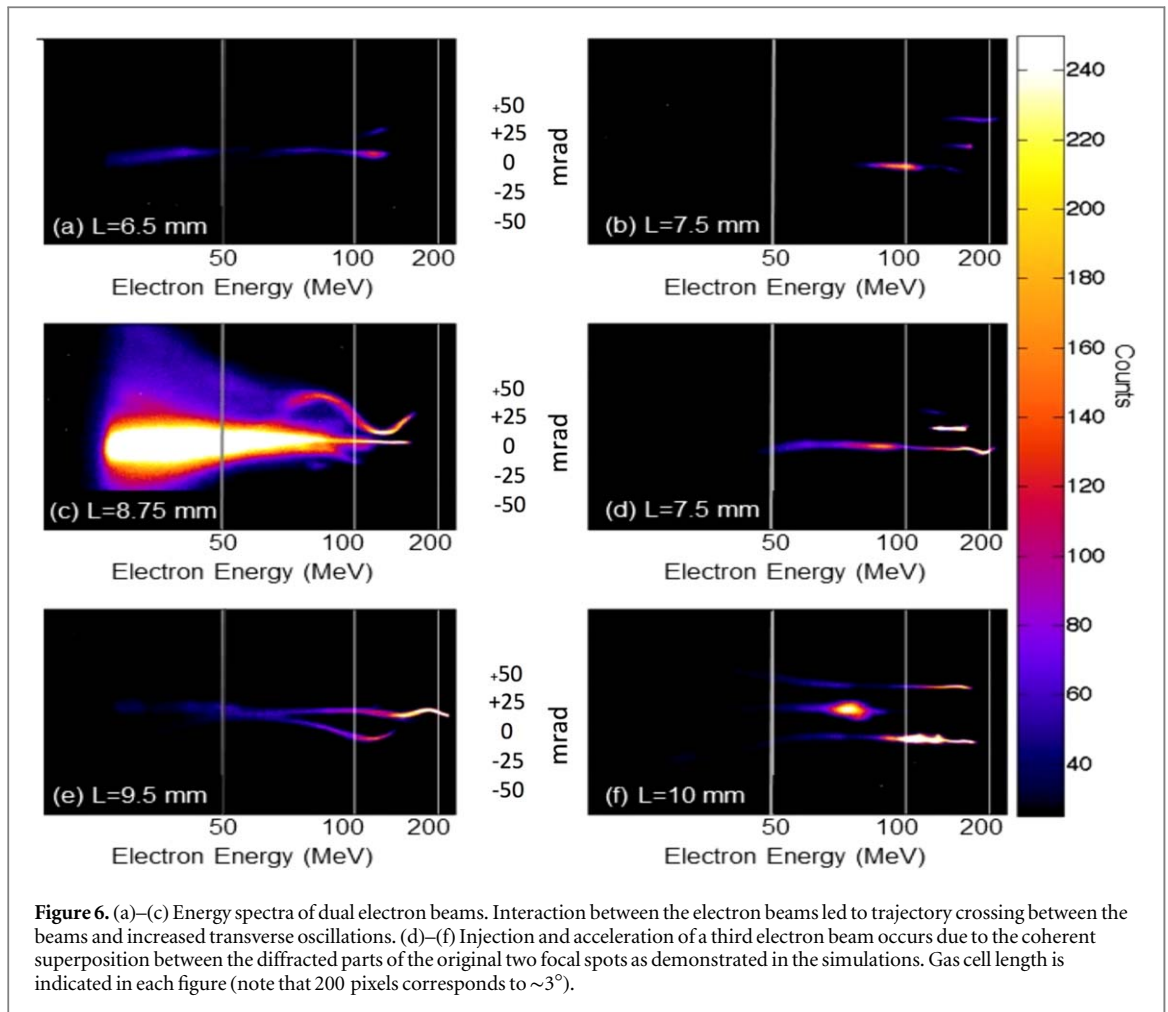


As mentioned earlier, the presence of dual electron beams appeared to delay the onset of beam loading in the wakefield. Figures 7(a) and (b) show the integrated electron signal for the 2.5% N₂ gas mixture and pure He gas, respectively, as a function of the electron density. All spectral images obtained using the π phase shift mirror, whether two electron beams were generated or not, are included in a data set ‘With π Mirror’ presented in figures 7(a) and (b). Similarly, all spectra obtained without the π phase shift mirror (i.e., images with only a single electron beam was generated) are designated as ‘No π Mirror’ in the two figures. Inspection of the data in figures 7(a) and (b) show a possible increase in the density which produced the highest charge in the dual beam case.

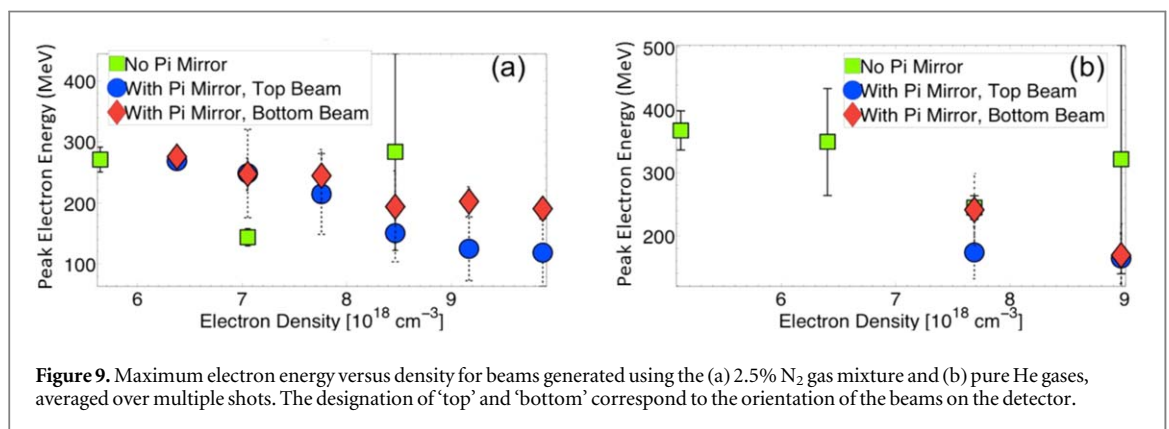
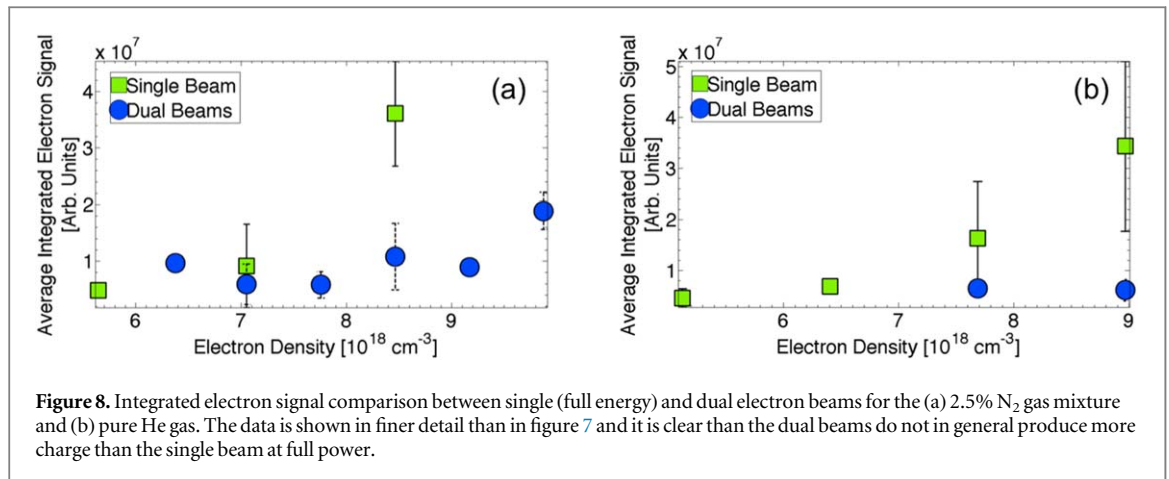
The integrated electron signal on the scintillating screen was characterized as a function of the electron density to determine if an increase in the total charge occurred in the case of distinct dual beams compared with a single beam. Figures 8(a) and (b) show the integrated signal from the single and dual beams generated using the 2.5% N₂ gas mixture and pure He gas, respectively. The circular data points result from images where two distinguishable electron beams were observed. Lower densities were below the injection threshold and thus do not produce any beams, while higher densities failed to produce distinct dual beams. It is clear from these experiments that the charge did not increase for the case of dual beams. In general, the charge contained in the dual beams is less than or at best equal to the charge contained in a combined single beam.

Experiments were also conducted to test whether electron beams could be generated using a single focal spot at half power, comparable to the power contained within each of the focal spots for the dual focus configuration. The energy spectra for these shots are represented by the diamond data points in figures 7(a) and (b) for the two gases. Overall, no significant injection was observed at half power (without a π -shift mirror). This trend suggests that injection of charge using dual focal spots is a result of interactions between the two wakefields. Efforts at producing electron beams at higher plasma densities at half power were also not successful and are not shown in the figures for clarity.

The maximum energy of the electron beams, defined as the highest energy with signal, is plotted in figure 9 for beams generated using the two gas types. For a given density, the energy of the single beam is higher than that of either dual beams because of the smaller laser intensity in the dual focal spots. The energies of the electron beams also decrease with increasing density as would be expected since both the dephasing and depletion lengths also decrease as density increases. The slight asymmetry in the energy between the top and bottom beams for the dual beams can be attributed to the uneven energy distribution in the two focal spots.



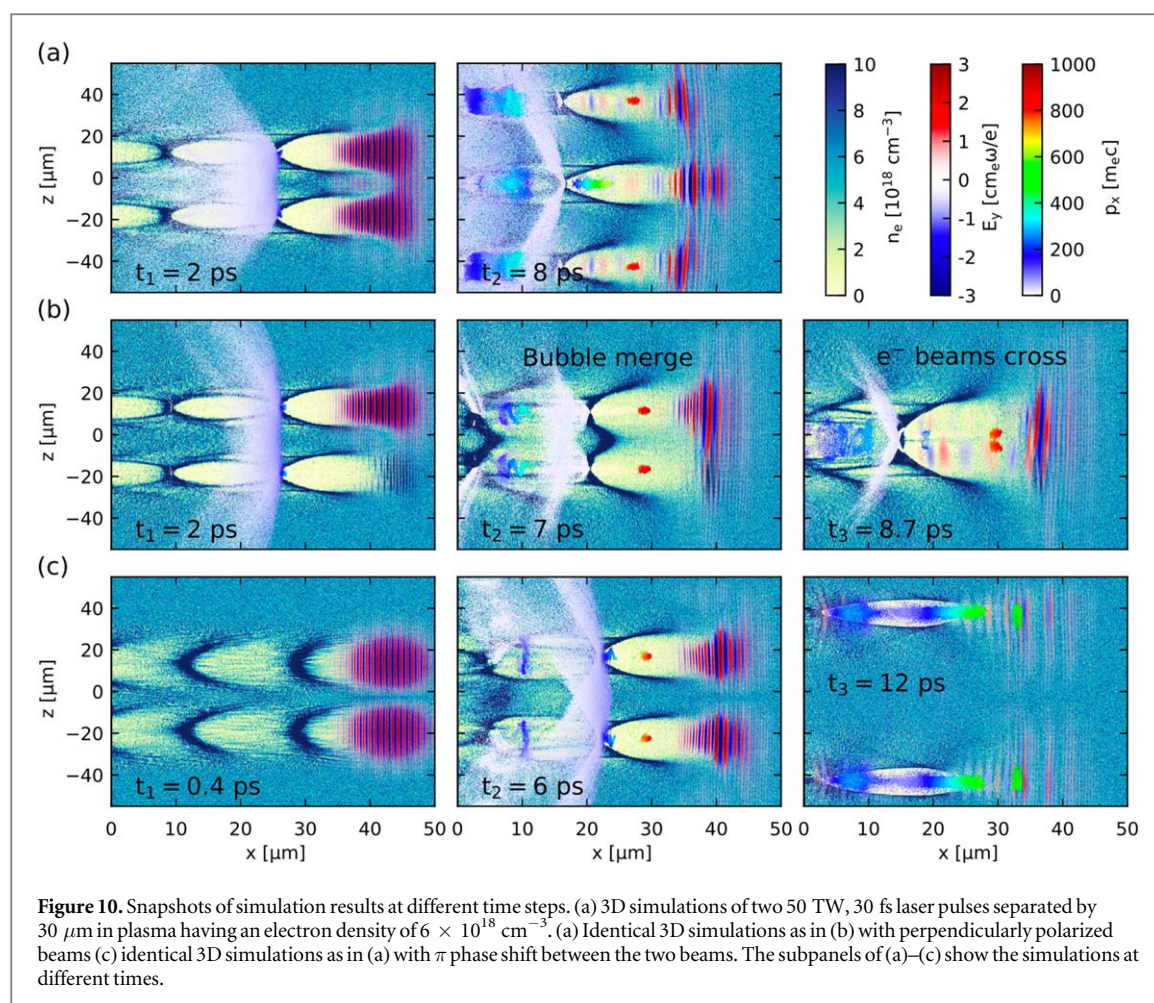
Particle-in-cell (PIC) simulations are required to better understand the interaction between the two wakefields and the role of the separation distance between the spots in generating multiple electron beams. Here we performed 3D simulations using the PIC code EPOCH [19] to model the interactions between the laser pulses. The simulation box with a moving window is $50 \mu\text{m} \times 80 \mu\text{m} \times 110 \mu\text{m}$ with $1250 \times 200 \times 275$ cells in x , y and z directions, respectively. There is one macro-particle in each cell with the ‘cold plasma’ condition. The plasma density is $6 \times 10^{18} \text{cm}^{-3}$ with a linear ramp for the first $50 \mu\text{m}$ of propagation. The two laser pulses in the simulations are identical with a laser power of 50 TW, a FWHM pulse duration of 30 fs and a FWHM spot size of $20 \mu\text{m}$ for each pulse. The laser pulses propagate in x which is also the direction of the moving window. They are both polarized in y except for the case with perpendicular polarization and are separated by $30 \mu\text{m}$ in z . We initially simulated two linearly polarized parallel pulses, and each pulse was seen to drive its own wakefield with electrons capable of being injected into the accelerating field of the adjacent wakefield bubble. When the



two pulses were closer to one another ($<20 \mu\text{m}$), they expelled electrons as a single, larger pulse and only one bubble is formed since the pulses propagate and self-focus as a unit. It should be noted that there is a reduced interaction between the two wakefields in the experiment versus the simulations, a result of larger experimental dual beam focal spot spacing.

However, in our simulations we also investigated the role of the laser phase and the polarization of the adjacent laser pulse. If a sufficient separation initially existed between two linearly polarized pulses with the same phase, then two wakefield bubbles are formed with a shared electron sheath boundary between them (figure 10(A)). After the pulses have self-focused, the bubbles remain clearly separated and trap and accelerate electrons independently. The charge in this case can be almost double that using a single beam case (i.e., with half the total laser energy). Those simulations also showed that the coherent superposition of the diffracted parts of the two focal spots can also create a third spot between the two that is intense enough to drive a third wakefield for an optimal separation. This is likely what has occurred in our experiments when a third electron beam is produced for long acceleration distances. From the simulations it is also very interesting to note that changing the polarization and the phase between beams (figures 10(B), (C)) dramatically changes the dynamics of the interaction as well as the number of electron beams and wakefields produced. In particular, with the π phase shift between the beams—no third wakefield structure or third electron beam is observed—which is similar to the data obtained from the vast majority of the data taken during these experiments. It is therefore likely that in the rare instances when three beams were observed in our experiments, that the phase mismatch between the two adjacent spots was not precisely π radians as in the EPOCH simulations. Unexpectedly when perpendicular polarizations are used in the simulations the adjacent wakefield bubbles merge—while the two electron beams are injected separately into the combined wakefield and undergo very large oscillations in the transverse direction to that of beam propagation (i.e., betatron oscillations).

In conclusion, it is clear from our experiments and simulations that the spot separation, inter-beam phase polarization and energy distribution play an important role in generating multiple high-energy beams and increasing the total charge. To control these factors in future experiments, a deformable mirror can be used to precisely manipulate the wavefront of the laser beam in order to obtain the optimal separation and maximum energy contained in the FWHM. Once these parameters are optimized, the corresponding emission of radiation [14] may also be controlled or increase accordingly—provided that the charge and peak energy of the electron



beams in each wakefield cavity is comparable to the charge and energy of an electron beam in a single wakefield cavity. By fine-tuning the focal spot parameters (and hence, the electron beam parameters), one could also manipulate the x-ray spectrum and also possibly decrease the x-ray beam divergence.

It is also clear that the number of wakefields can also be precisely controlled by using phase shifting mirrors and polarization control. These experiments showed that interaction between the wakefields can cause injection to occur for situations in which a single wakefield shows no significant injection. The combination of several such mirrors would result in a structure consisting of four or more focal spots, leading to the simultaneous generation of many wakefields. The region between these wakefields will provide a region with a charge maximum—similar to an ‘inverse’ nonlinear plasma bubble wakefield which can also potentially serve as an accelerating structure for positrons [20, 21].

Acknowledgments

This work was supported by AFRL, ARO (grant W911NF-16-1-0044), AFOSR (grant FA9550-16-1-0121) and DOE grant number DE-NA0002372.

ORCID iDs

K Krushelnick  <https://orcid.org/0000-0001-9116-9511>

References

- [1] Mangles S P D *et al* 2004 *Nature* **431** 535
- [2] Faure J, Gilneç Y, Pukhov A, Kiselev S, Gordienko S, Lefebvre E, Rousseau J-P, Burgy F and Malka V 2004 *Nature* **431** 541
- [3] Geddes C G R, Toth C, van Tilborg J, Esarey E, Schroeder C B, Bruhwiler D, Nieter C, Cary J and Leemans W P 2004 *Nature* **431** 538
- [4] Leemans W P, Nagler B, Gonsalves A J, Toth C S, Nakamura K, Geddes C G R, Esarey E, Schroeder C B and Hooker S M 2006 *Nat. Phys.* **2** 696

- [5] Hafz N A M et al 2008 *Nat. Photon.* **2** 571
- [6] Kneip S et al 2009 *Phys. Rev. Lett.* **103** 035002
- [7] Mangles S P D, Thomas A G R, Lundh O, Lindau F, Kaluza M C, Persson A, Wahlstrom C-G, Krushelnick K and Najmudin Z 2007 *Phys. Plasmas* **14** 056702
- [8] Faure J, Rechatin C, Norlin A, Lifschitz A, Glinec Y and Malka V 2006 *Nature* **444** 737
- [9] Geddes C G R, Nakamura K, Plateau G R, Toth C S, Cormier-Michel E, Esarey E, Schroeder C B, Cary J R and Leemans W P 2008 *Phys. Rev. Lett.* **100** 215004
- [10] Pak A, Marsh K A, Martins S F, Lu W, Mori W B and Joshi C 2010 *Phys. Rev. Lett.* **104** 025003
- [11] McGuffey C et al 2010 *Phys. Rev. Lett.* **104** 025004
- [12] Esarey E, Schroeder C B and Leemans W P 2009 *Rev. Mod. Phys.* **81** 1229
- [13] Wen M, Shen B, Zhang X, Ji L, Wang W, Xu J and Yu Y 2010 *Phys. Plasmas* **17** 103113
- [14] Corde S, Ta Phuoc K, Lambert G, Fitour R, Malka V and Rousse A 2013 *Rev. Mod. Phys.* **85** 1
- [15] Ma Y et al 2015 *Phys. Plasmas* **22** 083102
- [16] Kaluza M et al 2010 *Phys. Rev. Lett.* **105** 095003
- [17] Yanovsky V et al 2008 *Opt. Express* **16** 2109
- [18] Vargas M et al 2014 *Appl. Phys. Lett.* **104** 174103
- [19] Arber T D, Bennett K, Brady C S, Ramsay M G, Sircombe N J, Gillies P, Evans R G, Schmitz H, Bell A R and Ridgers C P 2015 *Plasma Phys. Control. Fusion* **57** 113001
- [20] Vieira J and Mendonca J T 2014 *Phys. Rev. Lett.* **112** 215001
- [21] Zhang G-B et al 2016 *J. Appl. Phys.* **119** 103101